

Contents lists available at [SciVerse ScienceDirect](http://www.sciencedirect.com)

Bioorganic & Medicinal Chemistry

journal homepage: www.elsevier.com/locate/bmc

Design, synthesis and biological evaluation of coumarin alkylamines as potent and selective dual binding site inhibitors of acetylcholinesterase

Marco Catto*, Leonardo Pisani, Francesco Leonetti, Orazio Nicolotti, Paolo Pesce, Angela Stefanachi, Saverio Cellamare, Angelo Carotti*

Dipartimento di Farmacia, Università degli Studi di Bari "Aldo Moro", via E. Orabona 4, Bari 70125, Italy

ARTICLE INFO

Article history:

Received 31 July 2012

Revised 25 October 2012

Accepted 29 October 2012

Available online xxx

Keywords:

Alzheimer's disease

Coumarin derivatives

Acetylcholinesterase

Dual binding site inhibitors

Selective cholinesterase inhibition

ABSTRACT

Acetylcholinesterase inhibitors (AChEIs) are currently the drugs of choice, although only symptomatic and palliative, for the treatment of Alzheimer's disease (AD). Donepezil is one of most used AChEIs in AD therapy, acting as a dual binding site, reversible inhibitor of AChE with high selectivity over butyrylcholinesterase (BChE). Through a combined target- and ligand-based approach, a series of coumarin alkylamines matching the structural determinants of donepezil were designed and prepared. 6,7-Dimethoxycoumarin derivatives carrying a protonatable benzylamino group, linked to position 3 by suitable linkers, exhibited fairly good AChE inhibitory activity and a high selectivity over BChE. The inhibitory potency was strongly influenced by the length and shape of the spacer and by the methoxy substituents on the coumarin scaffold. The inhibition mechanism, assessed for the most active compound **13** (IC₅₀ 7.6 nM) resulted in a mixed-type, thus confirming its binding at both the catalytic and peripheral binding sites of AChE.

© 2012 Elsevier Ltd. All rights reserved.

1. Introduction

Alzheimer's disease (AD) is a progressive neurodegenerative disorder associated with cognitive, functional and behavioral impairments.¹ It affects brain regions that control thought, memory and language, and evolves to a devastating status for patients and caregivers. Nearly 50 million people worldwide suffer from AD. Social and economic burdens of this disease are massive due to estimated direct and indirect annual costs of 100 billion dollars in patient care per year only in US. Despite the huge efforts of both industrial and academic scientists, the pathophysiological events causing the onset and progression of AD remain obscure and, as a consequence, the setup of appropriate pharmacological, disease-modifying therapies are still an unmet medical need.²

The current therapies for AD, yet symptomatic and palliative, rely mainly on the restoration of acetylcholine levels³ and on the partial antagonism of NMDA receptor⁴ (Chart 1). Marketed cholinergic drugs are inhibitors of acetylcholinesterase (AChE) often used in combination with diverse conventional drugs (e.g., antidepressants, antioxidants, and neuroprotectants).

AChE (EC 3.1.1.7) is a serine hydrolase located either in peripheral (muscles) and/or central nervous (cholinergic) system. Since

cholinergic transmission is involved in a variety of physiological systems, AChE is a pursued pharmacological target for treatment of several pathologies besides AD.⁵ AChE inhibitors (AChEIs) have therapeutic application in surgical anesthesia in the treatment of neuromuscular blockade,⁶ in myasthenia gravis⁷ and in glaucoma.⁸ Another cholinesterase, namely butyrylcholinesterase (BChE), is involved in metabolic degradation of acetylcholine and differs from AChE for tissue distribution and sensitivity to substrates and inhibitors (Chart 1).

The X-ray crystallographic structure of AChE solved at a high resolution for a large number of enzyme–ligand complexes⁹ reveals two main binding sites: the catalytic binding site, comprising the Ser–His–Glu catalytic triad, and the secondary/peripheral anionic binding site (PAS), connected by a deep, hydrophobic gorge. AChEIs can bind to the catalytic or the peripheral site, or, as in the case of dual binding site (DBS) inhibitors, to both the sites (e.g., donepezil, Chart 1). Ligand- and structure-based design has facilitated the discovery of potent and often selective AChE inhibitors, prepared by assembling two identical or different moieties through a linker of appropriate length and chemical nature.¹⁰ This straightforward strategy has been successfully applied to the design of AChE inhibitors potentially addressing additional targets,¹¹ according to multitargeted-ligand strategy, particularly promising in AD¹² as well as other multifactorial pathologies such as tumor diseases.¹³

In the course of our research aimed at the discovery of new molecular leads with therapeutic potential in neurodegenerative

* Corresponding authors. Tel.: +39 080 5442803; fax: +39 080 5442230 (M.C.); tel.: +39 080 5442782; fax: +39 080 5442230 (A.C.).

E-mail addresses: marco.catto@uniba.it (M. Catto), angelo.carotti@uniba.it (A. Carotti).

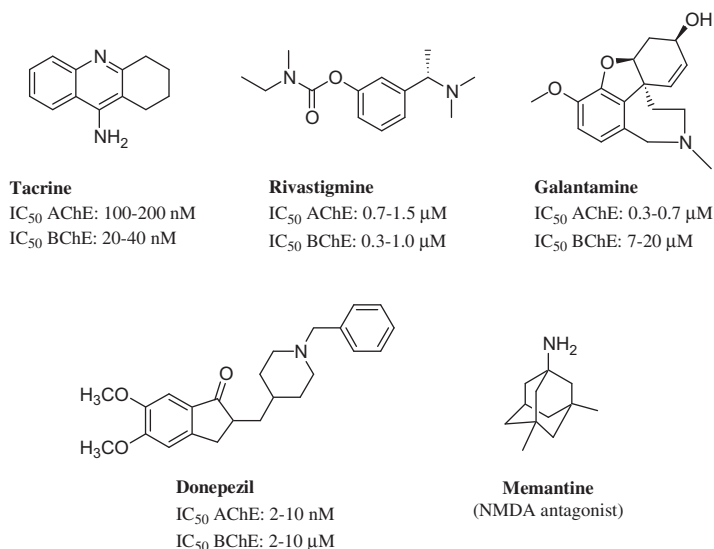


Chart 1. Marketed anti-AD drugs. For cholinergic drugs, inhibitory activity ranges on AChE and BChE are reported.

diseases (NDs), we have described several series of coumarin derivatives endowed with high AChE,¹⁴ monoamine oxidase (MAO)¹⁵ and dual MAO–AChE¹⁶ inhibitory activities. Other studies on coumarin derivatives as cholinesterase inhibitors, have been recently reviewed.¹⁷ Actually, coumarin scaffold represents a widely occurring, nature friendly privileged structure, whose functionalization is straightforward. With this skilled and easy chemistry in hand, we designed and prepared new potent and selective coumarin derivatives as cholinesterase inhibitors, in particular 6,7-dimethoxy-3-substituted coumarins, tethered to a benzylamine moiety placed at an appropriate distance from the heterocyclic ring.

In order to explore wide structure–activity relationships three readily available coumarin scaffolds were selected (Chart 2). The classic Ellman spectrophotometric test¹⁸ was then performed to assess the AChE and BChE inhibitory activities of the designed compounds, whose structures and ChE inhibition data are reported in Table 1.

2. Results and discussion

2.1. Chemistry

6,7-Dimethoxycoumarin-3-carboxylic acid **I**,¹⁹ 3-aminocoumarin **IIa**,²⁰ 3-amino-6,7-dimethoxycoumarin **IIb**,²¹ and 3-hydroxycoumarin derivatives **IIIa**,²² **IIIb**,²³ **IIIc**¹⁹ and **IIId**²¹ were prepared according to reported literature procedures. To achieve the final amides **1–3**, non-commercial amines **Va–c** were also prepared (Scheme 1). Amides and esters **1–8** were synthesized by condensation of **I** with suitable amines or alcohols through the use of coupling reagents (Scheme 2).

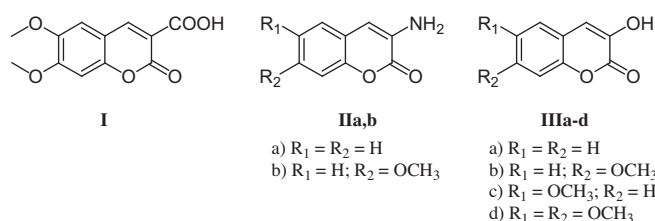


Chart 2. Coumarin scaffolds I–III.

Amides **9–12** were prepared from aminocoumarins **II** and commercial ω -chloroacyl chlorides, and subsequent nucleophilic substitution with benzylmethylamine (Scheme 3).

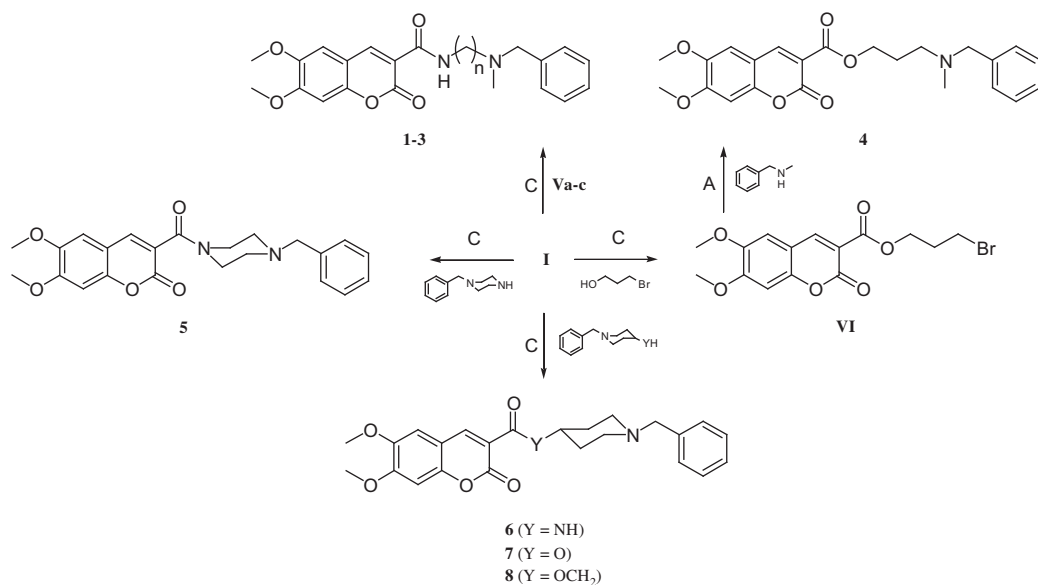
Coumarin **IIb** was also used as starting material for the synthesis of amide **13**, through the coupling with commercial *cis*-*N*-Boc-3-aminocyclohexanecarboxylic acid and final *N*-benzylation (Scheme 4). Compound **14** was prepared through two simple consecutive alkylation and nucleophilic substitution reactions from **IIIa** (Scheme 4).

Finally, derivatives **15–19** were prepared from 3-hydroxycoumarins **IIIa–d** by Mitsunobu condensation reaction with appropriate piperidiny alcohol (Scheme 5).

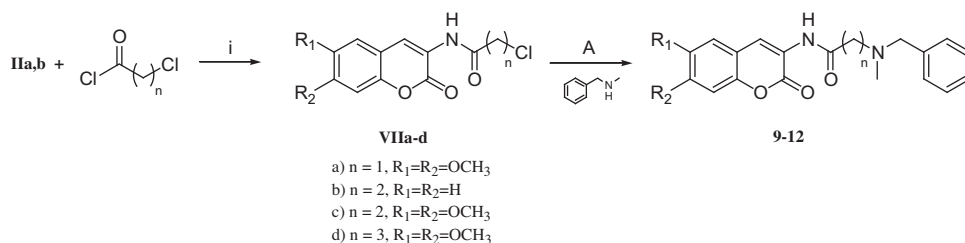
2.2. Cholinesterase inhibition

Inhibitory activities on AChE (from bovine erythrocytes) and BChE (from equine serum) were determined by the spectrophotometric method of Ellman¹⁸ and are reported in Table 1 as IC₅₀ (μM) or as percentage of inhibition at 10 μM.

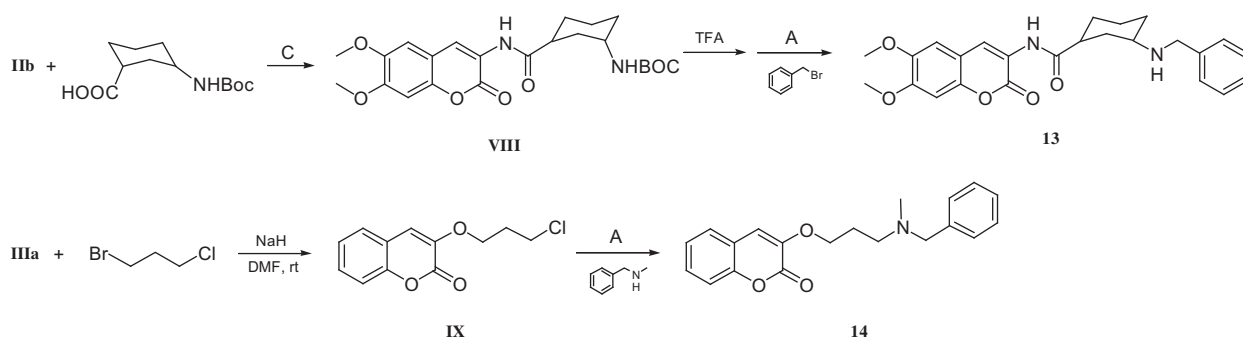
All compounds, with the exception of aminoethers **14**, **15** and **17**, acted as selective inhibitors of AChE over BChE, with IC₅₀s spanning from 66 μM of compound **10** to 7.6 nM of amide **13**, the latter showing inhibitory potency toward AChE very close to that of donepezil (4.2 nM). Amides **1–3** with a polymethylene bridge showed a significant increase of potency with the elongation of the linker. IC₅₀ significantly decreased from compound **1** (IC₅₀ = 9.0 μM, one of the less active compounds of the whole data set) to **2** (IC₅₀ = 86 nM), whilst **3** resulted among the most active inhibitors of the entire series examined (IC₅₀ = 21 nM). The small difference in the inhibitory activities of amide **2** and its isosteric ester **4** (86 vs 111 nM IC₅₀) contrasted indeed with the four-fold drop of inhibitory activity of compound **12**, an analogue of **2** bearing an inverted amide function. In comparison with the corresponding open-chain analogues **1** and **2**, piperazine and piperidine amides **5** and **6**, respectively, showed a slightly increased affinity. Even in this case, the small oversizing of linker from **5** to **6** led to a gain of affinity as high as two orders of magnitude (from 4.0 μM to 28 nM). Transformation of amide group of **6** into ester **7** resulted in an even higher potency (IC₅₀ 14 vs 28 nM), while a further elongation of the spacer in aminoester **8** led to a less active, but yet potent (IC₅₀ = 73 nM) and selective AChE inhibitor. Compound **9**, with a short methylene linker and aminoether **14** carrying a longer triethylene linker, showed low inhibitory potency. In the latter case, the lack of methoxy substituents in positions 6 and 7 of the coumarin ring



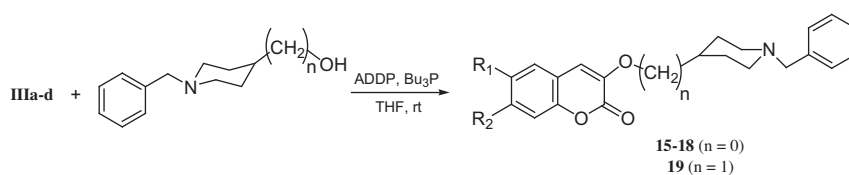
Scheme 2. Synthesis of compounds **1–8**. Reaction conditions: (A) as in Scheme 1; (C) DIC, HOBT, dichloromethane, rt.



Scheme 3. Synthesis of compounds **9–12**. Reaction conditions: (A) as in Scheme 1; (i) triethylamine, anhydrous THF, 0 °C.



Scheme 4. Synthesis of compounds **13** and **14**. Reaction conditions (A) and (C) as in Schemes 1 and 2, respectively.



Scheme 5. Synthesis of compounds **15–19**.

reported in Table 1 revealed a number of very potent compounds with AChE IC₅₀s as low as 30 nM (i.e., compounds **3**, **6**, **7**, **13** and **19**) with compound **13** being the most active and selective AChE inhibitor of the entire series of compounds examined

(IC₅₀ = 7.6 nM) and acting as a dual binding site inhibitor. Most inhibitors also showed high selectivity over BChE.

The outstanding inhibitory activity of compound **13**, retained also toward human AChE (IC₅₀ = 43 nM), deserves further investigation,

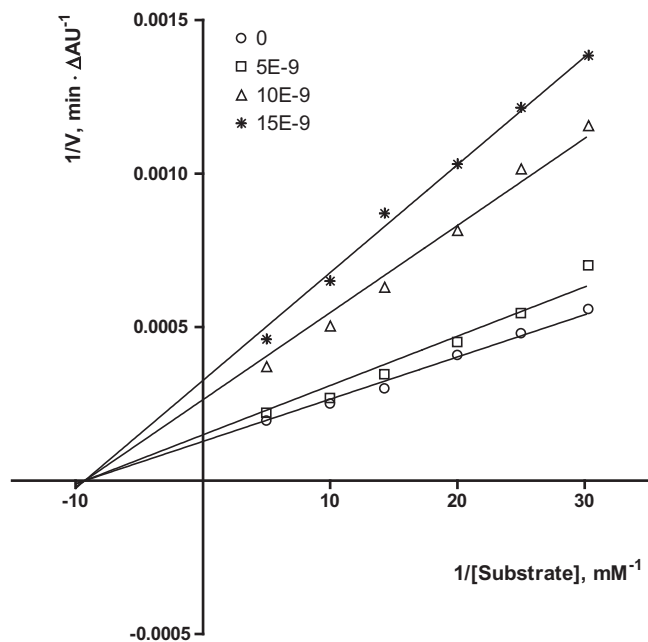


Figure 1. Lineweaver–Burk plot of inhibition kinetics of **13**: reciprocals of enzyme activity (bovine AChE) vs reciprocals of substrate (*S*-acetylthiocholine) concentration in the presence of different concentrations (0–15 nM) of inhibitor **13**.

firstly, in the evaluation of the inhibitory activities of each of the resolved enantiomers aiming at the discovery of a very potent eutomer and at the detection of the main enantioselective interactions at the AChE-binding sites. As an additional goal, compound **13** will be evaluated *in vitro* in the test of AChE-promoted beta-amyloid aggregation²⁵ and in *in vivo* models of AD. Data from these studies could give the definitive proof-of-concept of the potential of this coumarin derivative as a multipotent hit molecule for the treatment of AD.

4. Experimental section

4.1. Chemistry

Starting materials, reagents and analytical grade solvents were purchased from Sigma–Aldrich Europe (Steinheim, Germany). All reactions were routinely checked by TLC using Merck Kieselgel 60 F₂₅₄ aluminum plates and visualized by UV light or iodine. ¹H NMR spectra were recorded in the specified deuterated solvent at 300 MHz on a Varian Mercury 300 instrument. Chemical shifts are expressed in parts per million (δ) relative to the solvent signal and the coupling constants *J* are given in Hertz (Hz). The following abbreviations were used: s (singlet), d (doublet), t (triplet), qn (quintuplet), dd (double doublet), m (multiplet), br (broad signal); signals due to NH protons were located by deuterium exchange with D₂O. ESI-MS analyses were performed on an Agilent 1100 LC-MSD trap system VL. Chromatographic separations were performed on Biotage SP1 purification system using flash cartridges prepacked with KP-Sil™ 32–63 μ m, 60 Å silica; elution gradient was automatically set with “TLC plate measurement” mode, with dichloromethane/methanol (90:10 v/v) as TLC eluent. All the final compounds were recrystallized from ethyl alcohol. Melting points (mp) were taken on a Gallenkamp MFB 595010M apparatus (open capillary method) and are uncorrected. Elemental analyses were performed on a EuroEA 3000 analyser for C, H, N; experimental results agreed to within $\pm 0.40\%$ of theoretical values.

4.1.1. Synthesis of intermediate amines Va–c (Scheme 1)

Twenty five millimole of *N*-methylbenzylamine (3.03 g, 3.22 mL) and 30 mmol of ω -chloroalkanonitrile were refluxed with

30 mmol of anhydrous potassium carbonate (4.14 g) in 30 mL of anhydrous acetone for 3 h (reaction conditions A, Scheme 1). After cooling to rt and filtration, the solution was evaporated to dryness and the residue separated on SP1. A pale yellow oil was obtained that was identified through ESI-MS and NMR and used without further purification (**IVa–c**, yield 80–93%). A solution of 20 mmol of nitrile **IVa–c** in 50 mL of anhydrous THF was cannulated into a suspension of 1.25 g of lithium aluminum hydride (33 mmol) in 40 mL of anhydrous THF, kept under vigorous magnetic stirring at 0 °C (reaction conditions B). After 1 h the suspension was cautiously added with water until effervescence disappeared, then filtered and evaporated to dryness. Amines **Va–c** were obtained as pale yellow oils in a 61–84% yield, identified through ESI-MS and NMR and used without further purification.

4.1.2. Synthesis of compounds 1–8 (Scheme 2)

One twenty five milligram of 3-carboxycoumarin **1**¹⁹ (0.5 mmol) and 70 mg of diisopropylcarbodiimide (DIC; 0.55 mmol) were dissolved in 10 mL of anhydrous dichloromethane. After 3 min 74 mg of *N*-hydroxy-1,2,3-benzotriazole hydrate (HOBT; 0.55 mmol) were added (reaction conditions C), followed by 0.55 mmol of appropriate amine (**Va** for final compound **1**; **Vb** for **2**; **Vc** for **3**; *N*-benzylpiperazine for **5**; 4-amino-*N*-benzylpiperidine for **6**) or alcohol (3-bromopropanol for **VI**; *N*-benzyl-4-hydroxypiperidine for **7**; *N*-benzylpiperidin-4-ylmethanol for **8**). The reaction was stirred at rt until TLC monitoring showed the disappearance of **I** (4–8 h). The mixture was then filtered and evaporated to dryness, giving a residue that was separated on SP1 and crystallized.

4.1.2.1. 6,7-Dimethoxy-2-oxo-2H-chromene-3-carboxylic acid [2-(*N*-benzyl-*N*-methylamino)ethyl]amide (1). Yellow crystals, yield 63%, mp: 208–209 °C. ¹H NMR (DMSO-*d*₆) δ : 2.31 (s, 3H), 2.69 (s, 2H), 3.63 (br, 4H), 3.95 (s, 3H), 3.99 (s, 3H), 6.90 (s, 1H), 7.00 (s, 1H), 7.24–7.44 (m, 5H), 8.80 (s, 1H), 9.14 (br, 1H, exch.). Anal. Calcd for C₂₂H₂₄N₂O₅: C, 66.65; H, 6.10; N, 7.07. Found: C, 66.25; H, 6.43; N, 7.16.

4.1.2.2. 6,7-Dimethoxy-2-oxo-2H-chromene-3-carboxylic acid [3-(*N*-benzyl-*N*-methylamino)propyl]amide (2). Yellow crystals, yield 93%, mp: 144–145 °C. ¹H NMR (CDCl₃) δ : 1.83 (qn, *J* = 6.9 Hz, 2H), 2.22 (s, 3H), 2.48 (t, *J* = 6.9 Hz, 2H), 3.47–3.53 (m, 4H), 3.95 (s, 3H), 3.99 (s, 3H), 6.88 (s, 1H), 7.00 (s, 1H), 7.27–7.34 (m, 5H), 8.82 (s, 1H), 9.00 (br, 1H, exch.). Anal. Calcd for C₂₃H₂₈N₂O₅: C, 67.30; H, 6.38; N, 6.82. Found: C, 66.96; H, 6.05; N, 6.61.

4.1.2.3. 6,7-Dimethoxy-2-oxo-2H-chromene-3-carboxylic acid [4-(*N*-benzyl-*N*-methylamino)butyl]amide (3). Yellow crystals, yield 64%, mp: 142–143 °C. ¹H NMR (CDCl₃) δ : 1.63–1.71 (m, 4H), 2.45–2.55 (m, 5H), 3.45–3.47 (m, 4H), 3.95 (s, 3H), 3.99 (s, 3H), 6.89 (s, 1H), 7.00 (s, 1H), 7.30–7.40 (m, 5H), 8.82 (s, 1H), 8.86 (br, 1H, exch.). Anal. Calcd for C₂₄H₂₈N₂O₅: C, 67.91; H, 6.65; N, 6.60. Found: C, 67.95; H, 6.73; N, 6.82.

4.1.2.4. 6,7-Dimethoxy-2-oxo-2H-chromene-3-carboxylic acid (4-benzylpiperazin-1-yl)amide (5). Yellow crystals, yield 69%, mp: 203–204 °C. ¹H NMR (CDCl₃) δ : 2.48–2.54 (m, 4H), 3.40 (t, *J* = 4.2 Hz, 2H), 3.54 (s, 2H), 3.78 (t, *J* = 4.2 Hz, 2H), 3.92 (s, 3H), 3.96 (s, 3H), 6.84 (s, 1H), 6.86 (s, 1H), 7.29–7.32 (m, 5H), 7.85 (s, 1H). Anal. Calcd for C₂₃H₂₄N₂O₅: C, 67.63; H, 5.92; N, 6.86. Found: C, 67.38; H, 5.98; N, 6.90.

4.1.2.5. 6,7-Dimethoxy-2-oxo-2H-chromene-3-carboxylic acid *N*-(1-benzylpiperidin-4-yl)amide (6). Yellow crystals, yield 53%, mp: 189–190 °C. ¹H NMR (CDCl₃) δ : 2.08 (br, 4H), 2.39 (br, 2H), 2.91 (br, 2H), 3.70 (s, 2H), 3.94 (s, 3H), 3.99 (s, 3H), 4.05 (br, 1H),

6.89 (s, 1H), 6.99 (s, 1H), 7.36–7.38 (m, 5H), 8.79 (s, 1H), 8.87 (br, 1H, exch.). Anal. Calcd for $C_{24}H_{26}N_2O_5$: C, 68.23; H, 6.20; N, 6.63. Found: C, 67.86; H, 6.18; N, 6.98.

4.1.2.6. 6,7-Dimethoxy-2-oxo-2H-chromene-3-carboxylic acid (1-benzylpiperidin-4-yl)ester (7). Yellow crystals, yield 58%, mp: 147–148 °C. 1H NMR ($CDCl_3$) δ : 1.66 (br, 2H), 1.93 (br, 2H), 2.49 (br, 2H), 2.85 (br, 2H), 3.64 (s, 2H), 3.94 (s, 3H), 3.98 (s, 3H), 5.12 (br, 1H), 6.88 (s, 1H), 6.94 (s, 1H), 7.28–7.39 (m, 5H), 8.46 (s, 1H). Anal. Calcd for $C_{24}H_{25}NO_6$: C, 68.07; H, 5.95; N, 3.31. Found: C, 67.71; H, 6.07; N, 3.37.

4.1.2.7. 6,7-Dimethoxy-2-oxo-2H-chromene-3-carboxylic acid [(1-benzylpiperidin-4-yl)methyl]ester (8). Brown crystals, yield 57%, mp: 171–172 °C. 1H NMR ($CDCl_3$) δ : 1.90–2.17 (m, 5H), 2.60–2.67 (m, 4H), 3.97 (s, 3H), 3.99 (s, 2H), 4.00 (s, 3H), 4.15 (d, J = 3.3 Hz, 1H), 4.25 (d, J = 3.3 Hz, 1H), 6.79 (s, 1H), 7.45–7.47 (m, 3H), 7.61–7.63 (m, 2H), 7.67 (s, 1H), 9.16 (s, 1H). Anal. Calcd for $C_{25}H_{27}NO_6$: C, 68.64; H, 6.22; N, 3.20. Found: C, 68.30; H, 6.23; N, 3.32.

3-Carboxycoumarin **I** was reacted in the same reaction conditions C with 3-bromo-1-propanol. After SP1 separation, compound **VI** was obtained as a yellow solid and used without further purification (identification: ESI-MS and NMR; yield 64%). Reaction of **VI** with *N*-methylbenzylamine under the above reported conditions A yielded compound **4**, purified as above.

4.1.2.8. 6,7-Dimethoxy-2-oxo-2H-chromene-3-carboxylic acid [3-(*N*-benzyl-*N*-methylamino)propyl]ester (4). Brown crystals, yield 64%, mp: 97–98 °C. 1H NMR ($CDCl_3$) δ : 2.45–2.55 (m, 2H), 2.72 (s, 3H), 3.45–3.47 (m, 4H), 3.95 (s, 3H), 3.99 (s, 3H), 4.41 (t, J = 6.9 Hz, 2H), 6.85 (s, 1H), 7.03 (s, 1H), 7.43–7.45 (m, 3H), 7.62–7.64 (m, 2H), 8.63 (s, 1H). Anal. Calcd for $C_{23}H_{25}NO_6$: C, 67.14; H, 6.12; N, 3.40. Found: C, 66.74; H, 5.99; N, 3.17.

4.1.3. Synthesis of compounds 9–12 (Scheme 3)

Two twenty one milligram of 3-aminocoumarin **IIa**²⁰ or 3-amino-6,7-dimethoxycoumarin **II**²¹ (1.0 mmol) and 607 mg of triethylamine (0.84 mL; 6.0 mmol) were dissolved in 8 mL of anhydrous THF. A solution of 1.0 mmol of the appropriate ω -chloroacyl chloride (n = 1–3; see Scheme 3) in 2 mL of anhydrous THF was dropped through a dropping funnel under vigorous magnetic stirring in the reaction flask kept in ice-cold water. After 1 h the suspension was filtered and the solution evaporated to dryness, yielding ω -chloroamides **VIIa–d** in quantitative yield. Crude **VIIa–d** were reacted with *N*-methylbenzylamine in the above reported conditions A to give final compounds **9–12**. Compound **10** was crystallized as hydrochloride.

4.1.3.1. 2-(*N*-Benzyl-*N*-methylamino)-*N*-(6,7-dimethoxy-2-oxo-2H-chromen-3-yl)acetamide (9). Yellow crystals, yield 62%, mp: 177–178 °C. 1H NMR ($CDCl_3$) δ : 2.48 (s, 3H), 3.27 (s, 2H), 3.71 (s, 2H), 3.92 (s, 3H), 3.94 (s, 3H), 6.85 (s, 1H), 6.88 (s, 1H), 7.32–7.39 (m, 3H), 7.46–7.48 (m, 2H), 8.60 (s, 1H), 9.82 (br, 1H, exch.). Anal. Calcd for $C_{21}H_{22}N_2O_5$: C, 65.96; H, 5.80; N, 7.33. Found: C, 66.28; H, 5.57; N, 7.26.

4.1.3.2. 3-(*N*-Benzyl-*N*-methylamino)-*N*-(2-oxo-2H-chromen-3-yl)propionamide (10). White crystals, yield 62%, mp: 216–218 °C (dec.). 1H NMR ($DMSO-d_6$) δ : 2.63 (s, 3H), 3.11 (t, J = 6.0 Hz, 2H), 3.24 (t, J = 6.0 Hz, 2H), 4.31 (s, 2H), 7.26–7.34 (m, 3H), 7.29–7.70 (m, 9H), 8.56 (s, 1H), 10.05 (s, 1H, exch.), 10.91 (br, 1H, exch.). Anal. Calcd for $C_{20}H_{20}N_2O_3 \cdot HCl$: C, 64.42; H, 5.68; N, 7.51. Found: C, 64.80; H, 5.37; N, 7.16.

4.1.3.3. 3-(*N*-Benzyl-*N*-methylamino)-*N*-(6,7-dimethoxy-2-oxo-2H-chromen-3-yl)propionamide (11). White crystals, yield 63%, mp: 178–179 °C. 1H NMR ($CDCl_3$) δ : 2.36 (s, 3H), 2.57 (t, J = 6.0 Hz, 2H), 2.74 (t, J = 6.0 Hz, 2H), 3.68 (s, 2H), 3.92 (s, 3H), 3.94 (s, 3H), 6.85 (s, 1H), 6.89 (s, 1H), 7.26–7.34 (m, 3H), 7.40–7.43 (m, 2H), 8.64 (s, 1H), 11.07 (br, 1H, exch.). Anal. Calcd for $C_{22}H_{24}N_2O_5$: C, 66.65; H, 6.10; N, 7.07. Found: C, 66.40; H, 6.03; N, 7.07.

4.1.3.4. 4-(*N*-Benzyl-*N*-methylamino)-*N*-(6,7-dimethoxy-2-oxo-2H-chromen-3-yl)butyramide (12). Yellow crystals, yield 53%, mp: 104–105 °C. 1H NMR ($CDCl_3$) δ : 2.16 (br, 2H), 2.42–2.62 (m, 5H), 2.84 (br, 2H), 3.81–3.96 (m, 2H), 3.93 (s, 3H), 3.94 (s, 3H), 6.84 (s, 1H), 6.86 (s, 1H), 7.30–7.44 (m, 3H), 7.48–7.58 (m, 2H), 8.50 (br, 1H, exch.), 8.57 (s, 1H). Anal. Calcd for $C_{23}H_{26}N_2O_5$: C, 67.30; H, 6.38; N, 6.82. Found: C, 67.28; H, 6.57; N, 7.20.

4.1.4. Synthesis of compound 13 (Scheme 4)

3-Aminocoumarin **IIb** (2.7 mmol, 600 mg) and *cis*-*N*-Boc-3-aminocyclohexanecarboxylic acid (660 mg) were reacted in reaction conditions C to yield the desired coumarin intermediate **VIII** as a brown solid (57% yield; NMR and ESI-MS characterization). 446 mg of **VIII** (1.0 mmol) were dissolved in 20 mL of dichloromethane. The solution was cooled to 0 °C using an external ice bath, and trifluoroacetic acid (1.7 mL, 22 mmol) was added dropwise. The reaction solution was slowly allowed to warm to room temperature and stirred overnight. The mixture was then cooled to 0 °C and a 20% sodium carbonate aqueous solution (45 mL) was slowly added. The organic layer was evaporated to dryness and the resulting yellow solid was reacted with one equivalent of benzyl bromide (reaction conditions A) to produce, after purification, the final compound **13**.

4.1.4.1. *cis*-3-(Benzylamino)cyclohexanecarboxylic acid (6,7-dimethoxy-2-oxo-2H-chromen-3-yl)-amide (13). Yellow crystals, yield 51%, mp: 81–82 °C. 1H NMR ($DMSO-d_6$) δ : 1.18–1.36 (m, 2H), 1.72–1.90 (m, 3H), 2.30–2.08 (m, 3H), 2.66–2.82 (m, 1H), 2.94–3.10 (m, 2H), 3.78 (s, 3H), 3.82 (s, 3H), 4.10–4.20 (m, 1H), 7.06 (s, 1H), 7.26 (s, 1H), 7.38–7.44 (m, 3H), 7.44–7.60 (m, 2H), 8.57 (s, 1H), 9.05 (br, 1H, exch.), 9.62 (s, 1H, exch.). Anal. Calcd for $C_{25}H_{28}N_2O_5$: C, 68.79; H, 6.47; N, 6.42. Found: C, 68.48; H, 6.57; N, 6.20.

4.1.5. Synthesis of compound 14 (Scheme 4)

One sixty two milligram of 3-hydroxycoumarin **IIIa**²² (1.0 mmol) and 24 mg of sodium hydride (1.0 mmol) were dissolved in 5 mL of anhydrous DMF, then 0.79 g of 1-bromo-3-chloropropane (0.49 mL, 5.0 mmol) were added. The mixture was reacted at 120 °C for 1 h and poured into crushed ice. Extraction with diethyl ether (3 \times 10 mL) and evaporation of solvent to dryness gave **IX** as a brown solid, used as such for the subsequent reaction (yield 72%). 170 mg of **IX** (0.7 mmol) reacted with *N*-methylbenzylamine in the above reported conditions A to give, after chromatographic separation, pure compound **14**, which was finally crystallized as hydrochloride.

4.1.5.1. 3-[3-(*N*-Benzyl-*N*-methylamino)propoxy]-6,7-dimethoxy-2-oxo-2H-chromene (14). White crystals, yield 59%, mp (hydrochloride): 202–204 °C (dec.). 1H NMR ($CDCl_3$) δ : 2.08 (qn, J = 6.6 Hz, 2H), 2.25 (s, 3H), 2.59 (t, J = 6.6 Hz, 2H), 3.53 (s, 2H), 4.08 (t, J = 6.6 Hz, 2H), 6.82 (s, 1H), 7.18–7.43 (m, 9H). Anal. Calcd for $C_{20}H_{21}NO_3 \cdot HCl$: C, 66.75; H, 6.16; N, 3.89. Found: C, 66.60; H, 6.01; N, 4.22.

4.1.6. Synthesis of compound 15–19 (Scheme 5)

In a flame-dried flask flushed with Ar stream, 1.0 mmol of the appropriate 3-hydroxycoumarin **IIIa–d**^{19,21–23} were dissolved

together with 0.76 g of N,N'-azobis(dicarbonyldipiperidine) (ADDP; 3.0 mmol), 0.61 g of tributylphosphine (0.75 mL, 3.0 mmol) and the suitable alcohol (4-hydroxy-N-benzylpiperidine for compounds **15–18**; N-benzyl-4-piperidinemethanol for **19**) in 15 mL of anhydrous THF. After 24 h the reaction was filtered, evaporated to dryness and separated on SP1, affording title compounds that were finally crystallized.

4.1.6.1. 3-(1-Benzylpiperidin-4-yloxy)-2-oxo-2H-chromene (15). White crystals, yield 59%, mp: 141–142 °C. ¹H NMR (CDCl₃) δ: 1.88–2.04 (m, 4H), 2.35 (br, 2H), 2.79 (br, 2H), 3.56 (s, 2H), 4.42 (br, 1H), 6.87 (s, 1H), 7.21–7.40 (m, 9H). Anal. Calcd for C₂₁H₂₁NO₃: C, 75.20; H, 6.31; N, 4.18. Found: C, 74.89; H, 6.28; N, 4.36.

4.1.6.2. 3-(1-Benzylpiperidin-4-yloxy)-6-methoxy-2-oxo-2H-chromene (16). White crystals, yield 49%, mp: 151–152 °C. ¹H NMR (CDCl₃) δ: 1.75–1.86 (m, 2H), 2.35 (br, 2H), 2.74–2.76 (m, 4H), 3.52 (s, 2H), 3.82 (s, 3H), 4.51 (br, 1H), 7.00 (dd, J = 9.1 Hz, 3.0 Hz, 1H), 7.08 (d, J = 3.0 Hz, 1H), 7.20–7.37 (m, 7H). Anal. Calcd for C₂₂H₂₃NO₄: C, 72.31; H, 6.34; N, 3.83. Found: C, 71.94; H, 6.37; N, 3.94.

4.1.6.3. 3-(1-Benzylpiperidin-4-yloxy)-7-methoxy-2-oxo-2H-chromene (17). White crystals, yield 51%, mp: 127–128 °C. ¹H NMR (CDCl₃) δ: 1.84–1.95 (m, 2H), 2.03 (br, 2H), 2.33 (br, 2H), 2.78 (d, J = 6.0 Hz, 2H), 3.55 (s, 2H), 3.84 (s, 3H), 4.36 (br, 1H), 6.82 (s, 1H), 6.85 (d, J = 2.5 Hz, 1H), 6.89 (s, 1H), 7.25–7.34 (m, 6H). Anal. Calcd for C₂₂H₂₃NO₄: C, 72.31; H, 6.34; N, 3.83. Found: C, 71.93; H, 6.32; N, 4.12.

4.1.6.4. 3-(1-Benzylpiperidin-4-yloxy)-6,7-dimethoxy-2-oxo-2H-chromene (18). White crystals, yield 44%, mp: 62–63 °C. ¹H NMR (CDCl₃) δ: 1.86–2.10 (m, 2H), 2.12 (br, 2H), 2.43 (br, 2H), 2.84 (br, 2H), 3.62 (s, 2H), 3.90 (s, 3H), 3.91 (s, 3H), 4.35 (br, 1H), 6.78 (s, 1H), 6.82 (s, 1H), 6.90 (s, 1H), 7.27–7.41 (m, 2H), 7.42–7.70 (m, 3H). Anal. Calcd for C₂₃H₂₅NO₅: C, 69.86; H, 6.37; N, 3.54. Found: C, 69.93; H, 6.42; N, 3.32.

4.1.6.5. 3-[(1-Benzylpiperidin-4-yl)methoxy]-6,7-dimethoxy-2-oxo-2H-chromene (19). White crystals, yield 58%, mp: 60–61 °C. ¹H NMR (CDCl₃) δ: 1.82–2.15 (m, 2H), 2.24 (br, 2H), 2.45 (br, 2H), 2.93 (br, 2H), 3.62 (br, 2H), 3.91 (s, 3H), 3.92 (s, 3H), 3.96–4.06 (m, 2H), 4.20 (br, 1H), 6.81 (s, 1H), 6.82 (s, 1H), 6.83 (s, 1H), 7.41–7.45 (m, 3H), 7.62–7.66 (m, 2H). Anal. Calcd for C₂₄H₂₇NO₅: C, 70.40; H, 6.65; N, 3.42. Found: C, 70.63; H, 6.52; N, 3.33.

4.2. Biological tests

All materials were purchased from Sigma–Aldrich Europe. The inhibition assays of AChE from bovine erythrocytes (0.36 U/mg), and BChE from equine serum (13 U/mg), were run in phosphate buffer 0.1 M, at pH 8.0. Acetylthiocholine iodide was used as substrate and 5,5'-dithiobis(2-nitrobenzoic acid) (DTNB) as the chromophoric reagent.¹⁸ Inhibition assays were carried out on an Agilent 8453E UV–vis spectrophotometer equipped with a cell changer. Solutions of tested compounds were prepared starting from 10 mM stock solutions in DMSO that were diluted with aqueous assay medium to a final content of organic solvent always less than 1%. AChE inhibitory activity was determined in a reaction mixture containing 200 μL of a solution of AChE (0.415 U/mL in

0.1 M phosphate buffer, pH 8.0), 100 μL of a 3.3 mM solution of DTNB in 0.1 M phosphate buffer (pH 7.0) containing 6 mM NaHCO₃, 100 μL of a solution of the inhibitor (six to seven concentrations ranging from 1 × 10⁻¹⁰ to 1 × 10⁻⁴ M), and 500 μL of phosphate buffer, pH 8.0. After incubation for 20 min at 25 °C, acetylthiocholine iodide (100 μL of 5 mM aqueous solution) was added, and AChE-catalyzed hydrolysis was followed by measuring the increase of absorbance at 412 nm for 3.0 min at 25 °C. The concentration of compound which determined 50% inhibition of the AChE activity (IC₅₀) was calculated by non-linear regression of the response–log(concentration) curve, using GraphPad Prism® (v. 5). BChE inhibitory activity was assessed similarly using butyrylthiocholine iodide as the substrate. Kinetic studies were performed under the same incubation conditions, using six concentrations of substrate (from 0.033 to 0.2 mM) and four concentrations of inhibitor **13** (0–15 nM). Apparent inhibition constants and kinetic parameters were calculated within the 'Enzyme kinetics' module of Prism.

Acknowledgments

This work was supported by a grant from MIUR (Rome, Italy); PRIN project 20085HR5JK_005).

References and notes

1. Querfurth, H. W.; LaFerla, F. M. *N. N. Eng. J. Med.* **2010**, *362*, 329.
2. Corbett, A.; Smith, J.; Ballard, C. *Expert Rev. Neurother.* **2012**, *12*, 535.
3. Martorana, A.; Esposito, Z.; Koch, G. *CNS Neurosci. Ther.* **2010**, *16*, 235.
4. Tayeb, H. O.; Yang, H. D.; Price, B. H.; Tarazi, F. I. *Pharmacol. Ther.* **2012**, *134*, 8.
5. Orhan, I. E.; Orhan, G.; Gurkas, E. *Mini-Rev. Med. Chem.* **2011**, *11*, 836.
6. Bevan, D. R.; Donati, F.; Kopman, A. F. *Anesthesiology* **1992**, *77*, 785.
7. Meriggioni, M. N.; Sanders, D. B. *Lancet* **2009**, *8*, 475.
8. McKinnon, S. J.; Goldberg, L. D.; Peeples, P.; Walt, J. G.; Bramley, T. J. *Am. J. Manag. Care* **2008**, *14*, S20.
9. <http://www.rcsb.org/pdb/home/home.do>.
10. (a) Leonetti, F.; Catto, M.; Nicolotti, O.; Pisani, L.; Cappa, A.; Stefanachi, A.; Carotti, A. *Bioorg. Med. Chem.* **2008**, *16*, 7450; (b) Carlier, P. R.; Han, Y. F.; Chow, E. S. H.; Li, C. P. L.; Wang, H.; Lieu, T. X.; Wong, H. S.; Pang, Y. P. *Bioorg. Med. Chem.* **1999**, *7*, 351; (c) Camps, P.; Muñoz-Torrero, D. *Mini-Rev. Med. Chem.* **2001**, *1*, 163; (d) Gemma, S.; Gabellieri, E.; Huleatt, P.; Fattorusso, C.; Borriello, M.; Catalanotti, B.; Butini, S.; De Angelis, M.; Novellino, E.; Nacci, V.; Belinskaya, T.; Saxena, A.; Campiani, G. *J. Med. Chem.* **2006**, *49*, 3421.
11. (a) Bolognesi, M. L.; Matera, R.; Minarini, A.; Rosini, M.; Melchiorre, C. *Curr. Opin. Chem. Biol.* **2009**, *13*, 303; (b) Bolognesi, M. L.; Rosini, M.; Andrisano, V.; Bartolini, M.; Minarini, A.; Tumiatti, V.; Melchiorre, C. *Curr. Pharm. Des.* **2009**, *15*, 601.
12. Pisani, L.; Catto, M.; Leonetti, F.; Nicolotti, O.; Stefanachi, A.; Campagna, F.; Carotti, A. *Curr. Med. Chem.* **2011**, *18*, 4568.
13. Costantino, L.; Barlocco, D. *Curr. Med. Chem.* **2012**, *19*, 3353.
14. Pisani, L.; Catto, M.; Giangreco, I.; Leonetti, F.; Nicolotti, O.; Stefanachi, A.; Cellamare, S.; Carotti, A. *Chem. Med. Chem.* **2010**, *5*, 1616.
15. (a) Gnerre, C.; Catto, M.; Leonetti, F.; Weber, P.; Carrupt, P. A.; Altomare, C.; Carotti, A.; Testa, B. *J. Med. Chem.* **2000**, *43*, 4747; (b) Catto, M.; Nicolotti, O.; Leonetti, F.; Carotti, A.; Favia, A. D.; Soto-Otero, R.; Méndez-Álvarez, E.; Carotti, A. *J. Med. Chem.* **2006**, *49*, 4912; (c) Pisani, L.; Muncipinto, G.; Miscioscia, T. F.; Nicolotti, O.; Leonetti, F.; Catto, M.; Caccia, C.; Salvati, P.; Soto-Otero, R.; Méndez-Álvarez, E.; Passeleu, C.; Carotti, A. *J. Med. Chem.* **2009**, *52*, 6685.
16. Brühlmann, C.; Ooms, F.; Carrupt, P. A.; Testa, B.; Catto, M.; Leonetti, F.; Altomare, C.; Carotti, A. *J. Med. Chem.* **2001**, *44*, 3195.
17. Anand, P.; Singh, B.; Nirmal Singh, N. *Bioorg. Med. Chem.* **2012**, *20*, 1175.
18. Ellman, G. L.; Courtney, K. D.; Andres, V., Jr.; Featherstone, R. M. A. *Biochem. Pharmacol.* **1961**, *7*, 88.
19. Dean, F. M.; Robertson, A.; Whalley, W. B. *J. Chem. Soc.* **1950**, 895.
20. Kokotos, G.; Tzougraki, C. *J. Heterocycl. Chem.* **1986**, *23*, 87.
21. Jackson, Y. A. *Heterocycles* **1979**, *1995*, 9.
22. Shaw, K. N. F.; McMillan, A.; Armstrong, M. D. *J. Org. Chem.* **1956**, *21*, 601.
23. Offe, H. A.; Jatzkewitz, H. *Chem. Ber.* **1947**, *80*, 469.
24. Sugimoto, H.; Iimura, Y.; Yamamishi, Y.; Yamatsu, K. *J. Med. Chem.* **1995**, *38*, 4821.
25. Inestrosa, N. C.; Alvarez, A.; Perez, C. A.; Moreno, R. D.; Vicente, M.; Linker, C.; Casanueva, O. I.; Soto, C.; Garrido, J. *Neuron* **1996**, *16*, 881.